

# Numerical Simulation of Flow Processes in Extrusion Tools for Partly Crosslinked and Highly Filled Plastic Melts

Kalman Geiger<sup>1</sup>, Gerhard Alfred Martin<sup>2</sup>, Andreas Sobotta<sup>3</sup>

<sup>1</sup>Institute for Plastic Technology (IKT), University of Stuttgart, Stuttgart, Germany

<sup>2</sup>Plastic Process Technology Dr.-Ing. Martin GmbH, Nürnberg, Germany

<sup>3</sup>Ingenieur Office for Numerical Optimization Methods INO, Aachen, Germany

## Email address:

[kalman.geiger@ikt.uni-stuttgart.de](mailto:kalman.geiger@ikt.uni-stuttgart.de) (K. Geiger)

## To cite this article:

Kalman Geiger, Gerhard Alfred Martin, Andreas Sobotta. Numerical Simulation of Flow Processes in Extrusion Tools for Partly Crosslinked and Highly Filled Plastic Melts. *Composite Materials*. Vol. 3, No. 1, 2019, pp. 9-21. doi: 10.11648/j.cm.20190301.12

**Received:** October 22, 2018; **Accepted:** February 1, 2019; **Published:** February 28, 2019

---

**Abstract:** The complex flow behaviour of partly crosslinked or highly filled polymer melts will be described with a new heuristic flow law, which takes into account the pseudoplastic flow behaviour in the regime of the viscosity curve for low and for high shear rates. The CARPOW law is a combination of the often used power and Carreau law. It describes the flow behaviour of partly crosslinked or highly filled polymer melts for the shear rate ranges in extrusion and injection molding tools. The evaluation and the presentation of the rotational and the capillary rheometrical viscosity measurements are detailed described. For highly filled or for partly crosslinked plastic melts a new defined consistency parameter is defined. It characterizes the flow obstruction in the CARPOW law. Further the temperature invariant representation of the CARPOW law is shown. This new flow law is applied for a partly crosslinked and a highly filled polymer system. The design of the extrusion tools should consider the flow behaviour described by the CARPOW law. Only with this flow law the design of tooling in the case of partly crosslinked or highly filled polymer melts is correct. Two praxis relevant examples demonstrate the calculation for an extrusion die using this new flow law.

**Keywords:** Shear Flow, Heuristic Flow Law, Parameter Identification, Flow Obstruction, Extrusion Dies, Numerical Flow Simulation, Dynamic Crosslinked Thermoplastic Elastomers, Wood Plastic Compounds

---

## 1. Introduction

The characterization of the flow behaviour of plastic melts in the plastic compounding and the plastic processing operations is necessary for several reasons. The non-Newtonian flow behaviour of the plastic melts with fillers and reinforcing materials (glass, carbon or natural fibers), with partly crosslinked macrophases (thermoplastic elastomers) or with chemically modified macromolecules must be described with a suitably heuristic flow approach for the entire shear rate range. Only on the basis of such a flow approach is it possible to describe the flow processes in the flow channels with the required accuracy using 2D or 3D simulation models and to provide reliable bases for the design of extrusion and injection molding tools. Heuristic flow approaches should be a simple approximation equation. The mathematical structure should describe the flow behaviour over the entire shear

rate range. They should also contain parameters with physical meaning, so that they can be correlated with structural and recipe parameters of the plastic melt. The following article presents a new heuristic flow law to describe the pseudoplastic flow behaviour of partly crosslinked or highly filled plastic melts. The parameter identification of this approach is explained and a consistency parameter is introduced in order to describe the flow obstruction in such polymeric systems. The flow law is used in the simulation of the extrusion tools. New design and layout concepts are developed to fulfill the required design criteria for the extrusion tools. For a partly crosslinked and a wood plastic compound melt the flow channel of a sheet extrusion die is calculated. The absolute necessity of the new heuristic flow law is demonstrated for the correct rheological design of the sheet extrusion dies.

## 2. Heuristic Flow Law for the Viscosity Function of Highly Filled or Partly Crosslinked Plastic Melts

It is recommended to use a heuristic flow law that correctly reflects the flow behaviour over the entire shear rate range. It must describe the measured viscosity curve with a sufficient accuracy. A new flow law describing the non-Newtonian flow behaviour of partly crosslinked or highly filled polymer melts is presented in the following sections and its advantages and disadvantages are discussed.

### 2.1. The CARPOW Law

Figure 1 shows the basic course of a viscosity curve of highly filled or partly crosslinked plastic compounds.

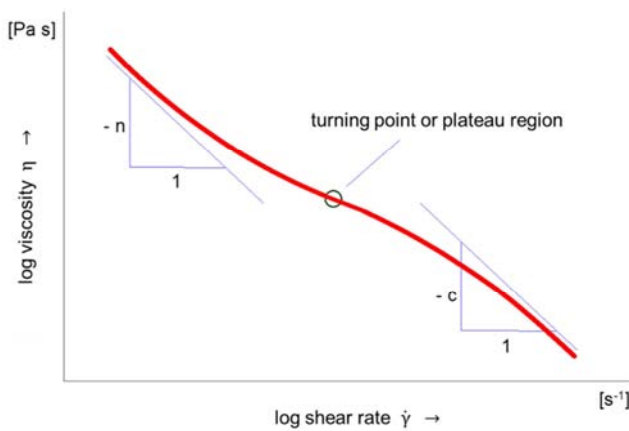


**Figure 1.** Viscosity curve of highly filled or partly crosslinked plastic melt in a double logarithmic plot, described with the CARPOW law (1) [11].

The flow behaviour in the range of high shear rates is characterized by pseudo-plasticity. In the range of low shear rates the viscosity increases with decreasing shear rates. A zero shear viscosity range is not existent. The two pseudoplastic flow areas are connected by a more or less pronounced plateau or a turning point area in the middle of the shear rate range.

A CARPOW law (1) is introduced to describe the viscosity curve shown in Figure 1 [11]. It is a combination of the CARreau law [3] and the POWer law by Ostwald / de Waele [1]:

$$\eta(\dot{\gamma}) = \frac{d}{\dot{\gamma}^n} + \frac{a}{(1+b \cdot \dot{\gamma})^c} \quad (1)$$

In equation (1) five parameters ( $d$ ,  $n$ ,  $a$ ,  $b$ , and  $c$ ) are available for an optimal approximation of the law to the measured viscosity values. The two flow exponents  $n$  and  $c$  are dimensionless,  $d$  has the dimension  $[\text{Pa s}^{1-n}]$ ,  $a$  has the dimension of the viscosity  $[\text{Pa s}]$  and  $b$  has the dimension of the time  $[\text{s}]$ . The exponents  $n$  and  $c$  can only assume physically meaningful values in the interval  $[0,1]$ . For the exponent  $n = 1$  is the parameter  $d$  exactly the yield stress of the investigated polymer system.

The CARPOW law (1) has the decisive advantage that it can be fitted to the measured viscosity curves of the filled or the partly crosslinked plastic melts. It has a high degree of flexibility

and accuracy over the required broad shear rate range. Equation (1) gives the asymptotic course of the viscosity curve for  $\dot{\gamma} \rightarrow 0$  and  $\dot{\gamma} \rightarrow +\infty$  correctly. The description of one-dimensional flow problems is possible with this approach only numerically. The parameter  $d$  has a from the flow exponent  $n$  dependent, physically non correct dimension. A scaling option for the shear rate and thus a conversion from  $d$  into a parameter with a physical correct dimension is provided by the turning point of the viscosity function. This detail is explained in section 2.1.4.

#### 2.1.1. The CARPOW Law for the Evaluation of the Rotational and the Capillary Rheometrical Viscosity Measurements

The complex shear viscosity  $\eta^*$  (more precisely, the magnitude of the complex shear viscosity  $|\eta^*|$ ) as a function of the angular frequency  $\omega$  can be approximated and represented on the basis of a selected heuristic flow approach. The shear viscosity  $\eta^*$  and the angular frequency  $\omega$  are set under the assumption of the Cox-Merz relation [9]. It is assumed as valid for the most filled and partly crosslinked polymers - at least approximately. The Cox-Merz relationship is usually accepted for the generation of complex polymer systems in plastic compounding and accordingly the complex shear viscosity is interpreted as the steady state shear viscosity. The plate-plate and the cone-plate rotational rheometer systems used to determine the complex shear viscosity do not require any correction steps as long as the oscillatory tests are carried out in the linear viscoelastic deformation range. For this reason oscillatory tests are the preferred rheological characterization method.

Capillary rheometer systems allow the determination of the viscosity function of a plastic melt in a wide shear rate range. A fundamental problem of the capillary rheometry is that there is an inhomogeneous shear rate distribution in the pressure gradient flow. Figure 2 shows the shear stress, the shear rate and the velocity distribution for a pressure gradient flow in a rectangular slit die.

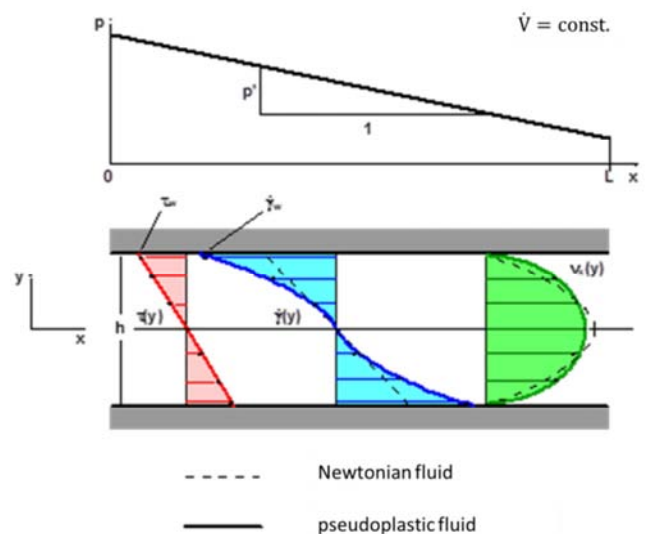


**Figure 2.** The shear stress, the shear rate and the velocity distribution in the rectangular slit die in a pressure gradient flow for Newtonian and pseudoplastic fluids.

The shear rate dependence of the viscosity of non-Newtonian fluids leads to the nonlinear shear rate distribution in the pressure gradient flow. In order to determine the "true" shear rate and the "true" shear viscosity for a measuring point of the "apparent" flow curve, the wall shear stress  $\tau_W = \tau (y = h / 2) = \tau$  is calculated from the pressure gradient. The "apparent" wall shear rate  $\dot{\gamma}_W^* = \dot{\gamma}^* (y = h / 2) = \dot{\gamma}_s$  is calculated from the volume rate and the slope of the "apparent" flow curve  $d\dot{\gamma}_s / d\tau$  has to be determined for the equation (2) according to the Weissenberg - Rabinowitsch evaluation step [7].

$$\dot{\gamma} = \left( \frac{2}{3} + \frac{1}{3} \cdot \frac{\tau}{\dot{\gamma}_s} \cdot \frac{d\dot{\gamma}_s}{d\tau} \right) \cdot \dot{\gamma}_s = \left( \frac{2}{3} + \frac{1}{3} \cdot \frac{d \lg \dot{\gamma}_s}{d \lg \tau} \right) \cdot \dot{\gamma}_s \quad (2)$$

Equation (2) is – in contrary to the widely used terminology – not a correction equation but a transformation rule for the determination of the geometry invariant "true" viscosity function of a non-Newtonian fluid. The slope  $d\dot{\gamma}_s / d\tau$  is obtained by approximating the "apparent" flow curve or the "apparent" viscosity curve with an equation that is continuously differentiable at each measuring point. Since the "apparent" viscosity curve already contains all the information about the flow behaviour of the fluid, it is useful to assume the heuristic flow approach even for the "apparent" viscosity curve. With this approach, the required slope  $d\dot{\gamma}_s / d\tau$  in equation (2) can be calculated. All further evaluation steps for the determination of the "true" shear rate and the parameters of the "true" viscosity function are then only algebraic conversions whose bases are derived for the new heuristic flow approach in the following sections.

**2.1.2. Asymptotics of the Weissenberg - Rabinowitsch Evaluation Equation**

The parameters of the "apparent" viscosity curve approach are numerically identified using a non-linear approximation method. The parameters for the viscosity function ("true" viscosity curve) are then determined using the parameters of the approach for the "apparent" viscosity curve. The asymptotic course of the "apparent" viscosity curve for  $\dot{\gamma}_s \rightarrow 0$  and  $\dot{\gamma}_s \rightarrow \infty$  is investigated and the conversion equations for the parameters are determined therefrom [5]. The exponents  $n$  and  $c$  in equation (1) are the same for the "true" and for the "apparent" viscosity curve. The parameter  $a$  in equation (1) is also the same for the "apparent" and for the "true" viscosity curve. This invariance of the parameter  $a$  due to the evaluation step (equation (2)) follows from the fact that the "true" and the "apparent" shear rates in the plateau region of the viscosity curve with  $d \lg \dot{\gamma}_s / d \lg \tau = 1$  are equal according to the equation (2). That will be also assumed for  $a$  in equation (1) if the viscosity curve does not show a plateau area at the turning point ( $d \lg \dot{\gamma}_s / d \lg \tau > 1$  in equation (2), figure 1). The approach used to approximate the "apparent" viscosity curve is formulated as follows:

$$\eta_s(\dot{\gamma}_s) = \frac{d_s}{\dot{\gamma}_s^n} + \frac{a}{(1+b_s \cdot \dot{\gamma}_s)^c} \quad (3)$$

The  $s$  indexed variables ( $\dot{\gamma}_s, \eta_s$ ) and the parameters  $b_s$  and  $d_s$  in equation (3) represent the "apparent" viscosity curve.

The asymptotic course of the CARPOW law (3) for the

"apparent" viscosity curve in the correction equation specified for the rectangular slit is investigated in equation (4) for  $\dot{\gamma}_s \rightarrow 0$  and  $\dot{\gamma}_s \rightarrow \infty$ :

$$\dot{\gamma} = \left( \frac{2}{3} + \frac{1}{3} \cdot \frac{\tau}{\dot{\gamma}_s} \cdot \frac{d\dot{\gamma}_s}{d\tau} \right) \cdot \dot{\gamma}_s = \left( \frac{2}{3} + \frac{1}{3} \cdot E(\dot{\gamma}_s) \right) \cdot \dot{\gamma}_s \quad (4)$$

The same limit value investigations are applied for the circular capillary with the correction equation (5):

$$\dot{\gamma} = \left( \frac{3}{4} + \frac{1}{4} \cdot \frac{\tau}{\dot{\gamma}_s} \cdot \frac{d\dot{\gamma}_s}{d\tau} \right) \cdot \dot{\gamma}_s = \left( \frac{3}{4} + \frac{1}{4} \cdot E(\dot{\gamma}_s) \right) \cdot \dot{\gamma}_s \quad (5)$$

The results of these limit investigations allow the conversion of the parameters  $b_s$  and  $d_s$  of the CARPOW law (3) for the "apparent" viscosity curve into the parameters  $b$  and  $d$  of the CARPOW law (1) for the "true" viscosity curve.

The asymptotic behaviour of equation (3) must be investigated for  $\dot{\gamma}_s \rightarrow 0$  and  $\dot{\gamma}_s \rightarrow \infty$ . The following limit values are obtained:

$$\lim_{\dot{\gamma}_s \rightarrow 0} E(\dot{\gamma}_s) = \frac{1}{1-n} \quad (6)$$

$$\lim_{\dot{\gamma}_s \rightarrow \infty} E(\dot{\gamma}_s) = \frac{1}{1-c} \quad (7)$$

With the equations (4) - (7) the bases for the conversion from the parameters  $b_s$  and  $d_s$  of the CARPOW law (3) ("apparent" viscosity) into the parameters  $b$  and  $d$  of the CARPOW law (1) ("true" viscosity) are created.

**2.1.3. Calculation of the Parameters of the "True" Viscosity Function**

The parameter  $d$  of the CARPOW law (1) is derived from the asymptotic behaviour of the equation (4) for  $\dot{\gamma}_s \rightarrow 0$  with equation (3) for the rectangular slit according to the equation:

$$d = \left( \frac{3-3 \cdot n}{3-2 \cdot n} \right)^{1-n} \cdot d_s \quad (8)$$

The parameter  $b$  of the CARPOW law (1) is obtained from the asymptotic behaviour of the equation (3) for  $\dot{\gamma}_s \rightarrow \infty$  with the equations (3) and (4):

$$b = \left( \frac{3-2 \cdot c}{3-3 \cdot c} \right)^{\frac{1}{c}-1} \cdot b_s \quad (9)$$

The "true" shear rates can be calculated on the basis of the equations (3) and (4) as follows:

$$\dot{\gamma} = \left( \frac{2}{3} + \frac{1}{3} \cdot \frac{a+d_s \cdot (1+b_s \cdot \dot{\gamma}_s)^c \cdot \dot{\gamma}_s^{-n}}{(1-n) \cdot d_s \cdot (1+b_s \cdot \dot{\gamma}_s)^c \cdot \dot{\gamma}_s^{-n} + a \cdot \frac{1+(1-c) \cdot b_s \cdot \dot{\gamma}_s}{1+b_s \cdot \dot{\gamma}_s}} \right) \cdot \dot{\gamma}_s \quad (10)$$

The calculation of the parameters of the CARPOW law (1) for the "true" viscosity function and the "true" shear rates with the CARPOW law (3) in the case of the circular capillary takes place according to equations (11) - (13):

$$d = \left( \frac{4-4 \cdot n}{4-3 \cdot n} \right)^{1-n} \cdot d_s \quad (11)$$

$$b = \left( \frac{4-3 \cdot c}{4-4 \cdot c} \right)^{\frac{1}{c}-1} \cdot b_s \quad (12)$$

$$\dot{\gamma} = \left( \frac{3}{4} + \frac{1}{4} \cdot \frac{a+d_s \cdot (1+b_s \cdot \dot{\gamma}_s)^c \cdot \dot{\gamma}_s^{-n}}{(1-n) \cdot d_s \cdot (1+b_s \cdot \dot{\gamma}_s)^c \cdot \dot{\gamma}_s^{-n} + a \cdot \frac{1+(1-c) \cdot b_s \cdot \dot{\gamma}_s}{1+b_s \cdot \dot{\gamma}_s}} \right) \cdot \dot{\gamma}_s \quad (13)$$

#### 2.1.4. Introduction of a Consistency Parameter $d_k$ into the CARPOW Law for Filled or Partly Crosslinked Plastic Melts

Figure 1 shows the principal course of the viscosity curve of a filled or a partly crosslinked plastic melt with the two characteristic pseudoplastic flow areas. The transition from the first flow region at low shear rates to the second one at high shear rates is marked by a turning point at  $\dot{\gamma} = \dot{\gamma}_{We}$ . This turning point of the viscosity curve can be determined with high accuracy if the two pseudoplastic flow ranges are ensured with many measured values  $\langle \eta; \dot{\gamma} \rangle$ . It also has a physical meaning: it marks the transition from plastic flow behaviour of the filled or the partly crosslinked melt to the pseudoplastic flow behaviour of the polymer matrix.

The turning point  $\eta_{We}$  ( $\dot{\gamma}_{We}$ ) of the viscosity curve can be used to normalize the shear rate in the CARPOW law (1). For the characterization of the flow obstruction and of the toughness of the filled or of the partly crosslinked system the consistency parameter  $d_k$  can be introduced. The first term of equation (1) can be rewritten with the normalization constant  $b_1$  as follows:

$$\frac{d}{\dot{\gamma}^n} = \frac{d_k}{(b_1 \cdot \dot{\gamma})^n} \quad (14)$$

In the equation (14)  $b_1$  has the dimension of the time and  $d_k$  the dimension of the viscosity. Setting  $b_1 = \dot{\gamma}_{We}^{-1}$  one gets  $d_k$  to

$$d_k = d \cdot \dot{\gamma}_{We}^{-n} \quad (15)$$

The turning point shear rate  $\dot{\gamma}_{We}$  in equation (15) is determined numerically from the double logarithmic represented CARPOW law (1). The second derivative of the equation (1) is analytically calculated and the zero point of this derivative is determined iteratively. Inserting  $\dot{\gamma}_{We}$  in equation (1) one obtains:

$$\eta(\dot{\gamma}) = d_k \cdot \left( \frac{\dot{\gamma}_{We}}{\dot{\gamma}} \right)^n + \frac{a}{(1+b \cdot \dot{\gamma})^c} \quad (16)$$

This normalization step for the low shear rates in the plastic flow range of the viscosity function in equation (16) allows to introduce a consistency parameter  $d_k$  for the filled or the partly crosslinked plastic melt and provides a basis for analyzing the influence of the filler concentration or the crosslinked fraction in the melt on their plastic flow behaviour at low shear rates. The CARPOW law (1) also offers the possibility of calculating flow processes in slow-flowing glass or natural fiber filled plastic melts during transfer molding and allow setting up optimization criteria for the tool design and the process control.

#### 2.1.5. Temperature Invariant Representation of the CARPOW Law

Rheological material functions can be displayed temperature invariant based on the Boltzmann time-temperature-superposition principle by introducing a

temperature shift factor  $a_T(T)$ . The flow exponents  $n$  and  $c$  of the CARPOW law (1) are assumed to be temperature invariant. After introducing the temperature dependent shift factor  $a_T(T)$  one obtains the equation

$$\eta(\dot{\gamma}|_T) = \frac{a_T^{1-n} \cdot d(T_0)}{\dot{\gamma}|_T^n} + \frac{a_T \cdot a(T_0)}{(1+a_T \cdot b(T_0) \cdot \dot{\gamma}|_T)^c} \quad (17)$$

With the shear rate at the turning point  $\dot{\gamma}_{We} = b_1^{-1}$  equation (17) can be represented as follows

$$\eta(\dot{\gamma}|_T) = \frac{a_T^{1-n} \cdot d_k(T_0)}{(b_1(T_0) \cdot \dot{\gamma}|_T)^n} + \frac{a_T \cdot a(T_0)}{(1+a_T \cdot b(T_0) \cdot \dot{\gamma}|_T)^c} \quad (18)$$

The temperature dependence of the shift factor  $a_T(T)$  in equation (18) can be described with the Arrhenius equation (preferred for semi-crystalline plastics)

$$a_T = \exp \left[ \frac{E}{R} \cdot \left( \frac{1}{T} - \frac{1}{T_0} \right) \right] \quad (19)$$

In the equation (19)  $E$  stands for the activation energy,  $R$  stands for the universal gas constant and  $T_0$  stands for a reference temperature selected in the underlying processing temperature range of the melt.

The parameters of a heuristic flow approach and the introduced temperature shift factor  $a_T(T)$  will be calculated numerically. For the non-linear CARPOW law (1) in the double logarithmic representation the parameters can be calculated with MATLAB [6]. The numerical Levenberg-Marquardt method is applied in order to minimize the least square fitting error for the optimization of the approach parameters with respect to the measured viscosity curve.

#### 2.2. Analytical Calculation of the Characteristic State Variables in the Shear Flow

The rheological flow law, whose parameters are identified by means of measured viscosity functions, allow the calculation of characteristic state variables in an one-dimensional shear flow. These flow types include the flow in the sheet dies, in the circular cylindrical annular gap, in the cylindrical full circle channel, etc. Default values are generally the flow channel geometry (the slit height  $h$ , the inner and outer diameter of the cylindrical annular gap  $\emptyset D_i$  and  $\emptyset D_a$ , the diameter of the full circle channel,  $\emptyset D$ ), the mass flow rate and the parameters of the flow approach. The "apparent" wall shear rate  $\dot{\gamma}_{ws}$  can be calculated directly from the volume flow rate according to the equations for the sheet shaped flow channels

$$\dot{\gamma}_{ws} = \frac{6 \cdot \dot{V}}{w \cdot h^2} \quad (20)$$

And for the circular shaped flow channels

$$\dot{\gamma}_{ws} = \frac{32 \cdot \dot{V}}{\pi \cdot D^2} \quad (21)$$

The relation of the parameters of the "true" and the "apparent" flow approach allows to calculate analytically the "true" shear rate with the flow rate parameters according to the equation (10) or (13). For "apparent" shear rates the equations (20) and (21) are valid for the slit and for the

circular flow channels respectively.

### 3. Examples for a Partly Crosslinked and a Highly Filled Plastic Melt

#### 3.1. Thermoplastic Elastomer

The mechanical and the elastic properties (tensile stress, elongation at break) of polypropylene (PP) - elastomer (EPDM) - blends (TPE) can be increased if the elastomer phase is dynamically crosslinked during compounding. The organosilane-grafted EPDM is mixed with the PP under the influence of the shear stress. The normal stresses in the superimposed shear and extensional flow in the closely intermeshing twin screws and the kneading elements of the co-rotating twin screw extruder ensure a good dispersive mixing [8]. PP is compounded with the organosilane grafted EPDM and the PP - EPDM - blends are compared concerning their viscosity in the following example.

The PP weight fraction in all PP - EPDM - blends to be compared is 35 weight %. The viscosity of the EPDM was much higher than that of the PP. At this high viscosity contrast the PP is dispersed in the physical blend with the ungrafted EPDM. The macroscopically extended PP is continuously distributed in the higher viscous EPDM

matrix. In the case of organosilane-grafted EPDM a phase inversion in the PP - EPDM - compound occurs during the dynamic crosslinking process in the kneading blocks of the twin screw extruder. The partly crosslinked EPDM particles are now dispersed in a continuous PP phase. Due to their high proportion by weight, the partly crosslinked EPDM particles represent a considerable flow obstruction in the PP - EPDM - blend.

Thermoplastic elastomers (TPE) can be generated as a physical blend with not crosslinked elastomer and with thermoplastic phases (co-continuous phase) or as a dynamically crosslinked blend with partly crosslinked elastomer particles in the thermoplastic matrix (dispersed phase). In the latter case, a thermoplastically processable TPE possessing the end properties of the elastomer component can be generated. The entropy elastic properties of the TPE can be influenced by the gel content of the partly crosslinked elastomer particles. Figure 3 shows the complex shear viscosity  $\eta^*(\omega)$  as function of the angular frequency  $\omega$  of the physical and the dynamically crosslinked PP - EPDM - blend. The complex viscosity function  $\eta^*(\omega)$  is interpreted as the steady state shear viscosity function under the assumption of the Cox-Merz rule [9]. The viscosity curves are calculated with the CARPOW law (1).

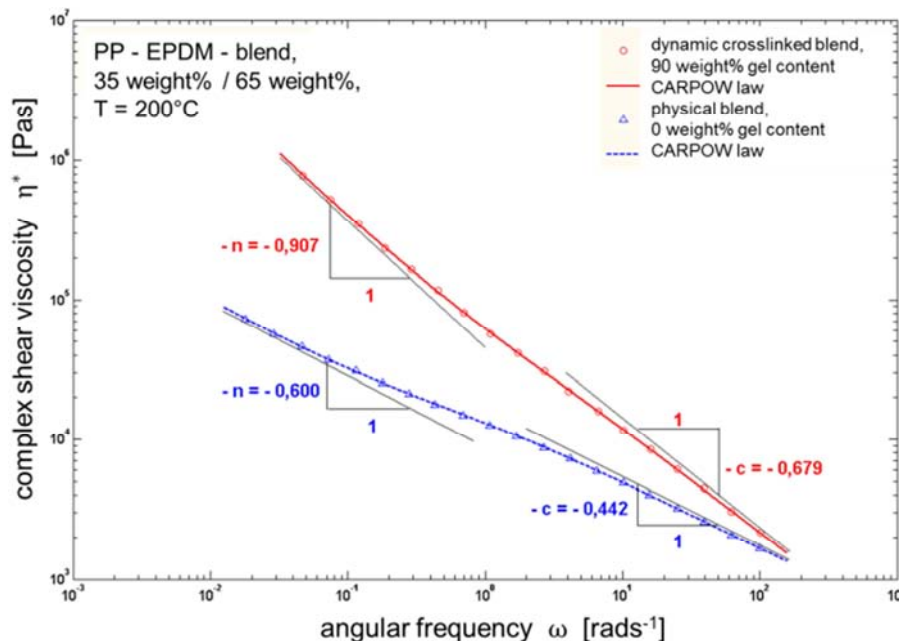


Figure 3. Complex shear viscosity  $\eta^*(\omega)$  as function of the angular frequency  $\omega$  of a physically and a dynamically crosslinked PP - EPDM - blend.

The physical blend has the characteristic complex shear viscosity function of a non-linear viscoelastic fluid with a light flow obstruction at low angular frequencies. The  $\eta^*(\omega)$  curve of the dynamically crosslinked blend exhibits in the low angular frequency region nearly the slope  $-1$  due to the plastic flow behaviour of a solid body with a yield stress. The flow behaviour of the physically and the dynamically crosslinked PP - EPDM - blend is determined by the continuous PP phase in the

region of high angular frequencies. The polypropylene can then be considered as the matrix of a dispersion with crosslinked rubber particles (gel fraction: 90 weight %). The slightly increased viscosity of the compound compared to the viscosity of the matrix polymer can be explained with the flow obstruction of these elastic "fillers". The turning point of the  $\eta^*(\omega)$  curve indicates the transition from the plastic flow of a solid body (interacting rubber particles) to the pseudoplastic

flow behaviour determined by the PP matrix.

The gel content in the dynamically crosslinked EPDM particles influences the formation of the morphology of the PP - EPDM - blend and thus affects the flow behaviour of the melt.

This gel dependent change of the flow behaviour is demonstrated in the  $\eta^*(\omega)$  curves in Figure 4.

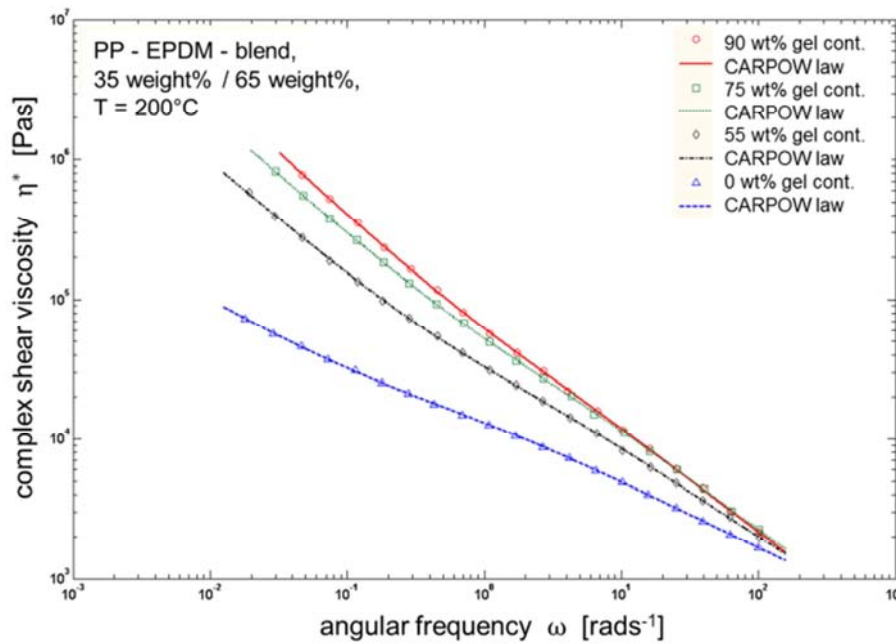


**Figure 4.** The complex shear viscosity  $\eta^*(\omega)$  as function of the angular frequency  $\omega$  of the dynamically crosslinked PP - EPDM - blends with different gel content.

As the gel content of the crosslinked EPDM increases the plastic flow behaviour in the region of low angular frequencies becomes more and more pronounced. Table 1 contains the parameters of the CARPOW law (1), the complex shear viscosity  $\eta_{w_e}^*$  at the turning point, the angular frequency  $\omega_{w_e}$  at the turning point and the consistency parameter  $d_k$  (equation (15)). As the gel content increases,

the turning point moves towards higher angular frequencies and a significant increase of the consistency parameter can be seen. This confirms the change of the flow behaviour of the dynamically crosslinked PP - EPDM - blends in the sense of an elastic solid body with yield stress (the first flow exponent  $n$  in table 1).

**Table 1.** The parameters of the CARPOW law (1), the complex shear viscosity at the turning point, the angular frequency at the turning point and the consistency parameter of the PP - EPDM - blends with different gel content (PP / EPDM weight fraction: 35% / 65%,  $T_0 = 200^\circ\text{C}$ ).

PP - EPDM - blend gel cont. wt[%]	parameters of the CARPOW law					turning point of the $h^*(\omega)$ - function		Consistency parameter
	$d$ [Pa s <sup>-n</sup> ]	$n$ [-]	$a$ [Pa s]	$b$ [s]	$c$ [-]	$h_{w_e}^*$ [Pa s]	$\omega_{w_e}$ [rad s <sup>-1</sup> ]	$d_k$ [Pa s]
0	5674	0,60	10001	0,98	0,44	14556	0,53	2262
55 - 60	20233	0,84	15990	0,48	0,59	21555	2,08	10974
75 - 80	38709	0,87	16979	0,36	0,67	26298	2,84	15678
90	48355	0,91	16994	0,37	0,68	24903	3,55	15322

In this empirical way the quantification of the dependence of the parameters of the CARPOW law (1) on the gel content is possible. It permits the prediction of the expected flow behaviour of a dynamically crosslinked PP - EPDM - blend with the gel content. An estimation of the expected gel content from the  $\eta^*(\omega)$  curves of the partly crosslinked blend is available if the rheological properties of a reference sample with a defined gel content is known.

### 3.2. Wood Plastic Compounds (WPC)

Polymeric materials are often modified with fillers in order to improve their mechanical properties, to reduce the material costs or to open new ways for the processing of low price semi-finished products. Wood plastic

compounds (WPC) are such polymeric materials. WPC's are composed of a matrix of thermoplastic polymer filled with wood flour. The materials can be processed with high mass contents of the wood flour in the polymeric matrix by profile extrusion. The semi-finished WPC-profiles can be applied for example for the furniture industry [14, 16]. The investigation and the description of the rheological properties of the WPC's are subject to recent research. Laufer *et al* [15] investigate the influence of the wood flour content on the flow behavior of LDPE and PP filled with different lignocel particles. The influence of the lignocel content is shown in the consistency parameter of the WPC and a shift factor as function of the wood flour content is introduced for the consistency parameter of the

applied power law.

The CARPOW law (1) gives a good possibility to the precise description of the flow behavior of WPC melts in a wide shear rate and shear stress range. Figure 5 shows the temperature invariant viscosity master curve for a PP based WPC melt with 50 weight [%] wood flour content at the reference temperature  $T_0 = 180^\circ\text{C}$ . The viscosity

curves are measured with the capillary rheometer using a rectangular slit die. Table 2 includes the five parameters of the CARPOW law (1): the activation energy for the temperature shift factor (eq. (18)), the shear rate and the viscosity at the turning point of the viscosity curve and the consistency parameter (eq. (14)) of the PP based WPC melt at the reference temperature  $T_0 = 180^\circ\text{C}$ .

**Table 2.** The parameters of the CARPOW law (1): the activation energy of the temperature shift, the steady state shear viscosity at the turning point, the shear rate at the turning point and the consistency parameter of for a polypropylen (PP) based WPC-melt with 50 weight % wood flour content.

WPC	parameters of the CARPOW law					turning point of the $h(\dot{\gamma})$ - function		consistency parameter
	$d[\text{Pa s}^{1-n}]$	$n[-]$	$a[\text{Pa s}]$	$b[\text{s}]$	$c[-]$	$E[\text{kJ kmol}^{-1}]$	$\dot{\gamma}_{wc}[\text{rad s}^{-1}]$	$d_k[\text{Pa s}]$
	17063	0,45	1156	0,21	0,74	33523	29489	0,72
								19780

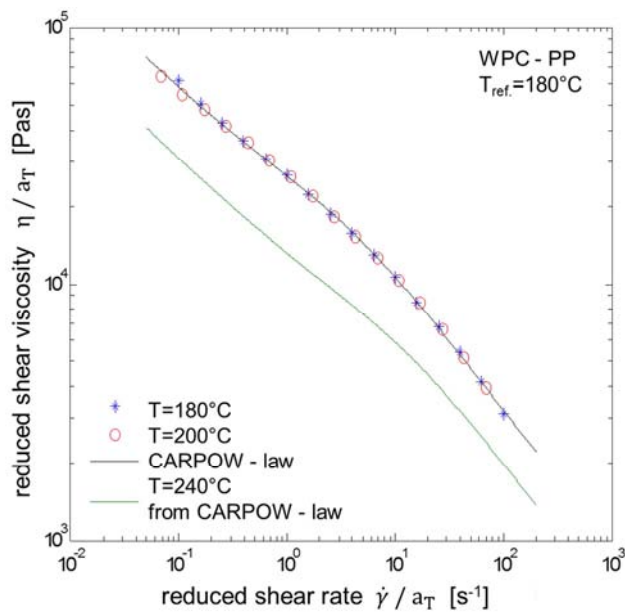


**Figure 5.** The steady state shear viscosity  $\eta(\dot{\gamma})$  as function of the shear rate  $\dot{\gamma}$  for a polypropylen (PP) based WPC-melt with 50 weight % wood flour content.

The shear rate at the turning point is low and corresponds to the shear induced dissolution of the wood particle network. The temperature shift factor of the PP based WPC melt is not influenced by the wood particles also for such high wood particle content and corresponds to that of the unfilled polypropylen matrix.

## 4. Rheological Design of Flow Channels in Extrusion Tools

### 4.1. Basic Design

When designing extrusion tools the basic design is done with analytical calculation methods. In the next step you use the numerical calculation methods. The objectives of the calculation are a good cleaning of the walls of the tool (cleaning flow), a reasonable pressure drop and a uniform melt distribution. The temperature increase of the melt should be as low as possible. In many cases a relaxation zone with low shear and normal stresses in the melt is recommended. In addition, you can cool the melt or extrudate

multi-layered semi-finished plastic products. Depending on the application in the medical technology or in the usual plastic market and for a large number of polymers, additional requirements for the design of extrusion tools can apply.

### 4.2. Cleaning Flow

Rapid color changes and short residence times for thermally sensitive polymers (PVC) are important in the most applications. The wall shear rates and the wall shear stresses in the flow channels are essential. The aim is to ensure the minimum wall shear stresses in which the molecules are peeled off from the wall by the flow. For this one chooses empirically verified stress values. From the production practice one knows the conditions in which a tool has a long lifetime and no deposits (burns) build up. This flow conditions are the right values for the wall shear stresses [10, 12].

### 4.3. Relaxation

In a relaxation zone the macromolecules relax from the stretched to the entangled state. There are applications in which a largely uniform state of stress and orientation should be present when the melt enters the land length of the extrusion tool. In the relaxation zone the shear rate should be below the critical shear rate  $\dot{\gamma}_{crit}$ . The macromolecules can relax and entangle. The necessary relaxation time is approximately the reciprocal value of the critical shear rate  $\dot{\gamma}_{crit}$ . (transition from the Newtonian to the pseudoplastic flow range of the viscosity curve). Relaxation zones should be designed in extrusion tools [10]. In the case of high molecular weight polymers (high molecular weight polyolefins), the critical shear rate is lower than the usual processing shear rates. For highly filled plastic melts or partly crosslinked polymer systems it lacks completely. In these cases the relaxation zones are extremely long.

### 4.4. 3D Calculation and Optimization of Rheologically Correct Designed Extrusion Tools Using the Example of a Sheet Die

The numerical application of the CARPOW law (1) is investigated by means of the flow simulations in extrusion tools. The results of the numerical calculations by using the CARPOW law (1) differ considerably from applying the Carreau law. For filled or partly crosslinked melts the

distribution of the melt in the flow channel is highly influenced by the higher viscosities in the low shear rate regions.

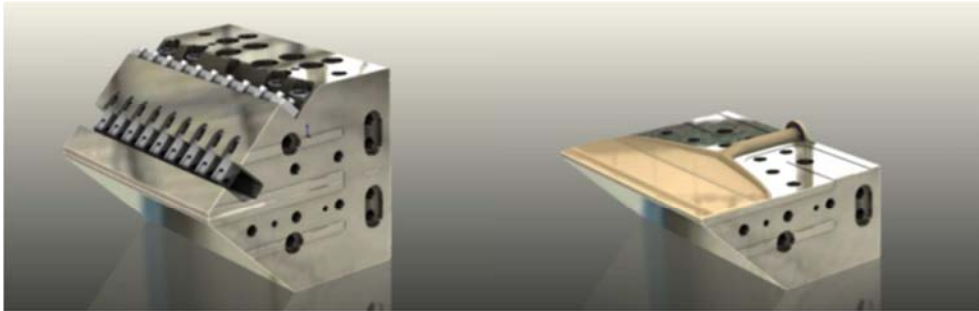


Figure 6. Left: the sheet die, right: the flow channel.

Table 3. The geometry of the sheet die and the process parameters.

material	PP - EPDM - blend
mass flow	150 kg/h
mass temperature	200°C
width of the sheet die	480 mm
zero-radius	14 mm
dam length	75 mm
dam gap	4 mm

The flow simulations are performed under the following assumptions:

1. The flow is steady state and laminar,
2. The thermodynamic characteristics (specific heat capacity, thermal conductivity, density) are constant,
3. The channel wall is adiabatic,
4. The applied rheological model is the CARPOW law (1) without the temperature shift (isothermal simulation conditions),

#### 4.4.1. 3D CAD / CFD Model Definition

Figure 6 shows a sheet die. Table 3 contains the geometry and the process parameters of the die.

5. The entry temperature and the entry velocity are constant,
6. The melt sticks at the channel walls,
7. The wall shear stresses are maintained constant (cleaning flow).

#### 4.4.2. Partly Crosslinked PP - EPDM - Blend with Different Gel Content

##### Pressure distribution

The pressure distribution in the tool is the result of the selected gaps in the flow channel (figure 7). It becomes clear that only with a reasonable choice of the geometry of the flow channel a low pressure drop can be achieved. The maximal and unavoidable pressure drop occurs in the land length. Its geometry determines the extruded product. With a well-designed tool the pressure drop is lower than one would expect from experience - although the walls are well cleaned.

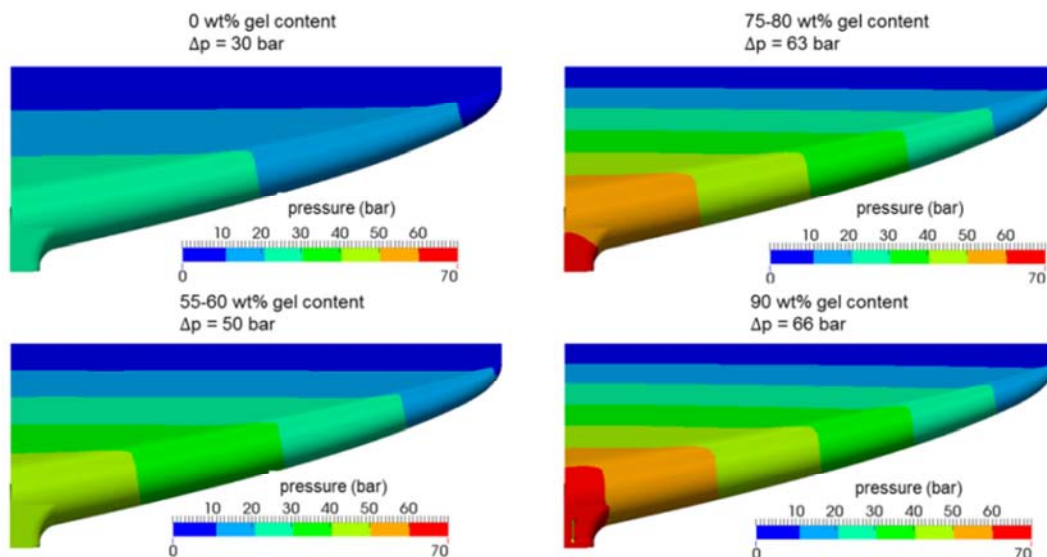


Figure 7. The pressure drop in the sheet die for different gel contents of the PP - EPDM - blend,  $T = 200^{\circ}\text{C}$ .

##### Velocity distribution at the sheet die exit

The velocity in the channel and over the width of the sheet die provides information about the quality of the design (figure 8). The velocity deviation across the width of the die

is 20% in the middle of the dam and 70% at the edge. The distribution of the velocity over cross section of the dam shows a transition to a plug flow with the increasing gel content.

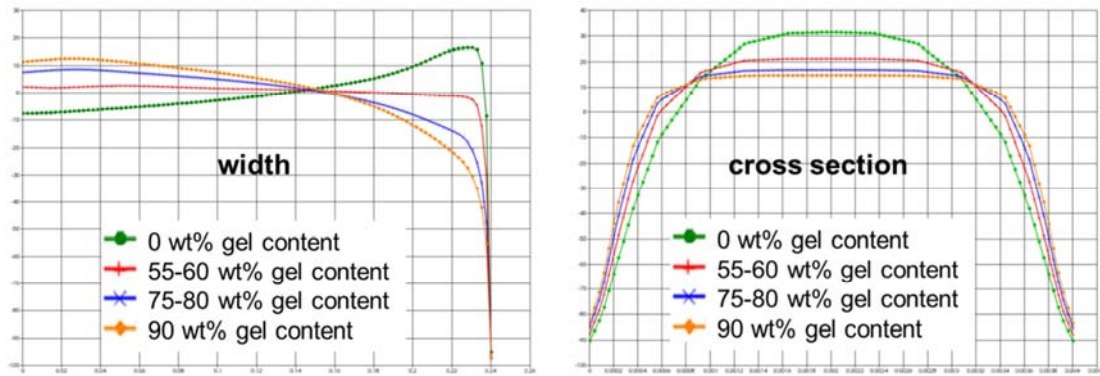


Figure 8. The velocity distribution at the exit of the sheet die for different gel contents of the PP - EPDM - blend,  $T = 200^{\circ}\text{C}$ , left: over the width of the sheet die, right: over the cross section of the dam.

Shear rates at the channel wall

The shear rate in the flow channel and at the channel walls is calculated with the CARPOW law (1). For each gel content the shear rate results are different (figure 9). The

channel cross sections are selected to obtain the desired shear rates. Since the finite volume method is based on a network it is important to start with a well-chosen channel geometry.

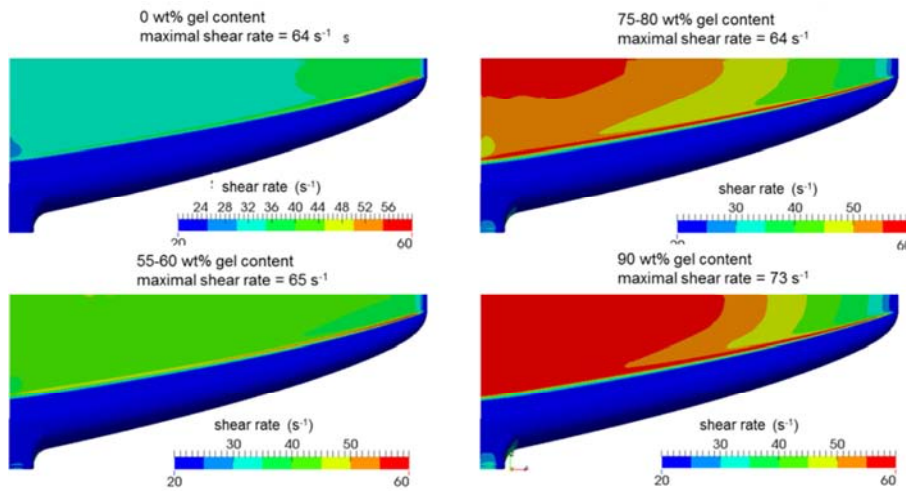


Figure 9. The shear rate distribution in the sheet die for different gel contents of the PP - EPDM - blend,  $T = 200^{\circ}\text{C}$ .

Figure 10 shows the viscosity curves marked in the relevant shear rate range for each case.

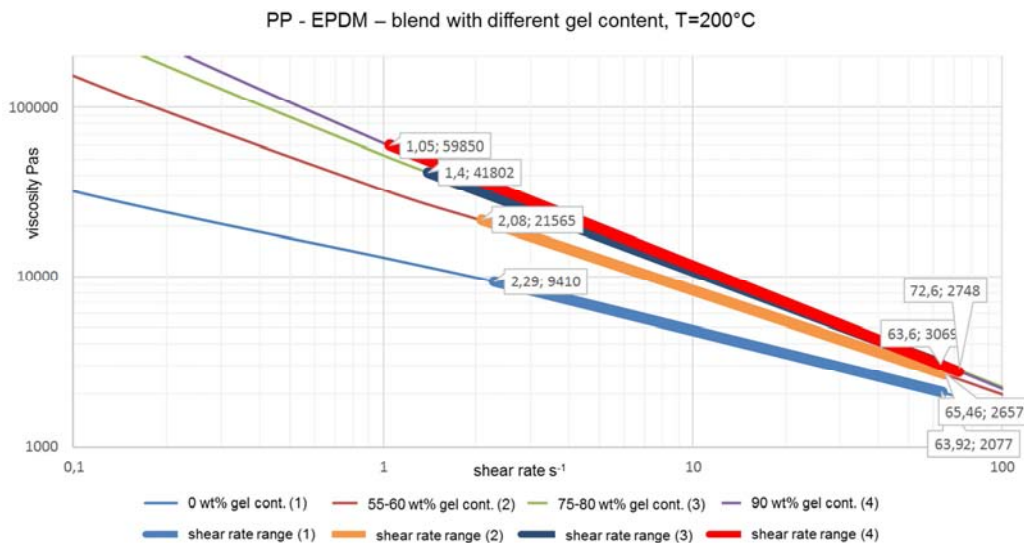


Figure 10. The viscosity curves for different gel contents of the PP - EPDM - blend. The relevant shear rate range for the sheet die is marked,  $T = 200^{\circ}\text{C}$ .

Velocity distributions at the exit of the sheet die with a relaxation zone and the land length

To optimize quality of the extrudate a relaxation zone is necessary. The land length improves the velocity distribution over the die width (figure 11). For the broad spectrum of gel contents a broad velocity distribution at the exit of the sheet

die would be expected. With the calculation method of constant shear rates at the flow channel walls one obtains narrow deviations:

1. 10% in the middle of the sheet die
2. 14% at the edge of the sheet die

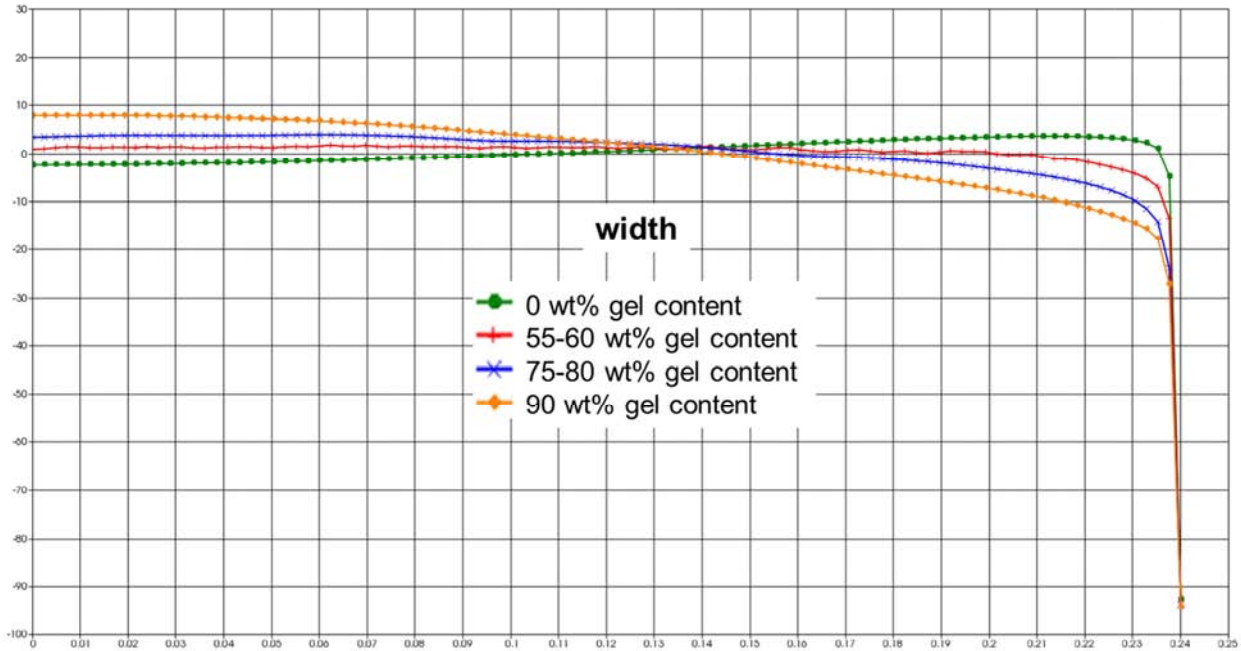


Figure 11. Velocity distribution at the exit of the sheet die across the width for different gel contents of the PP - EPDM - blend,  $T = 200^{\circ}\text{C}$ .

#### 4.4.3. Wood Plastic Compounds (WPC)

The same type of sheet die (figure 6) is used to check the design concept for the PP based WPC melt with 50 weight % wood flour content.

Figure 12 shows the viscosity curve marked in the relevant shear rate range corresponding to the processing conditions.

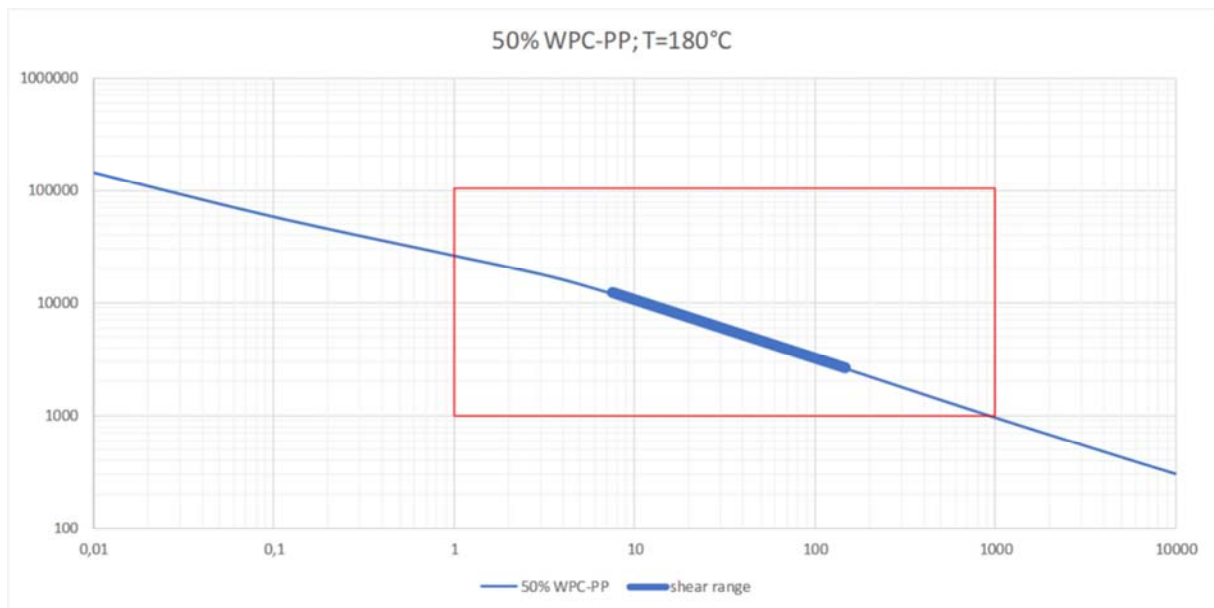


Figure 12. The viscosity curve for the PP based WPC melt with 50 weight % wood flour content. The relevant shear rate range for the sheet die is marked,  $T = 180^{\circ}\text{C}$ .

The calculated distribution of the pressure, the wall shear rate, the wall shear stress and the temperature at the wall are presented in figure 13. The required extrusion pressure (upper left side in figure 13) is high corresponding to the high viscosity of the WPC-PP melt at low shear rates. The wall shear rate distribution (upper right side in figure 13) and

the wall shear stress distribution (lower left side in figure 13) are high and uniformly in a broad central area. Due to the high wall shear rates and wall shear stresses the temperature increase at the die wall (lower right side in figure 13) is in the central area also high.

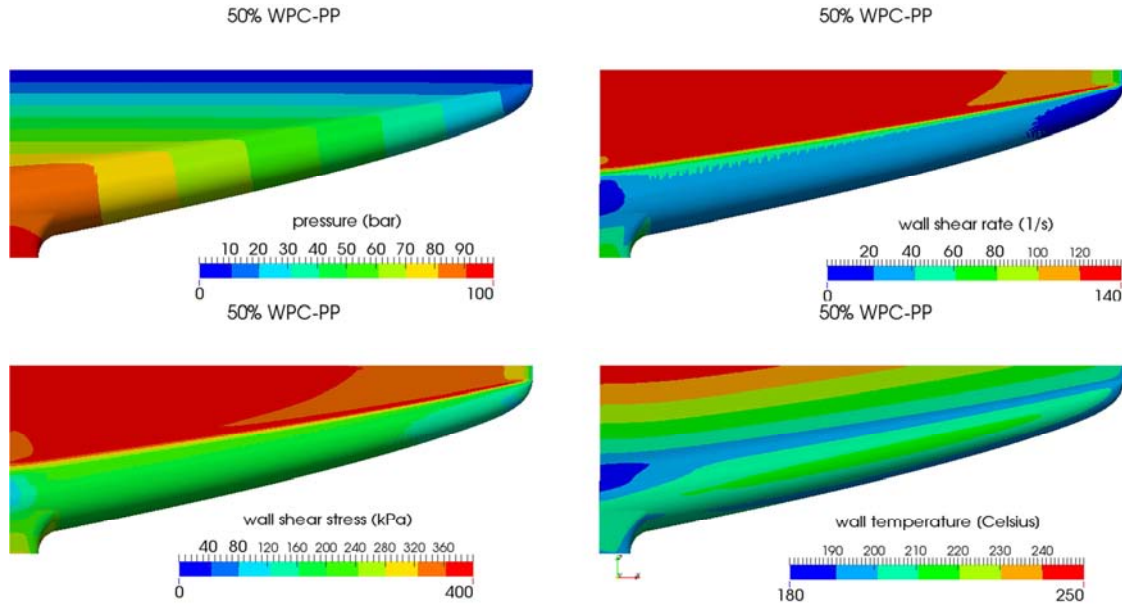


Figure 13. The distribution of the pressure, of the wall shear rate, of the wall shear stress and of the temperature at the wall of the sheet die for the PP based WPC melt with 50 weight %,  $T = 180^{\circ}\text{C}$ .

Figure 14 shows the distribution of the temperature, of the shear rate, of the viscosity, of the velocity and of the shear stress in the cross section of the sheet die.

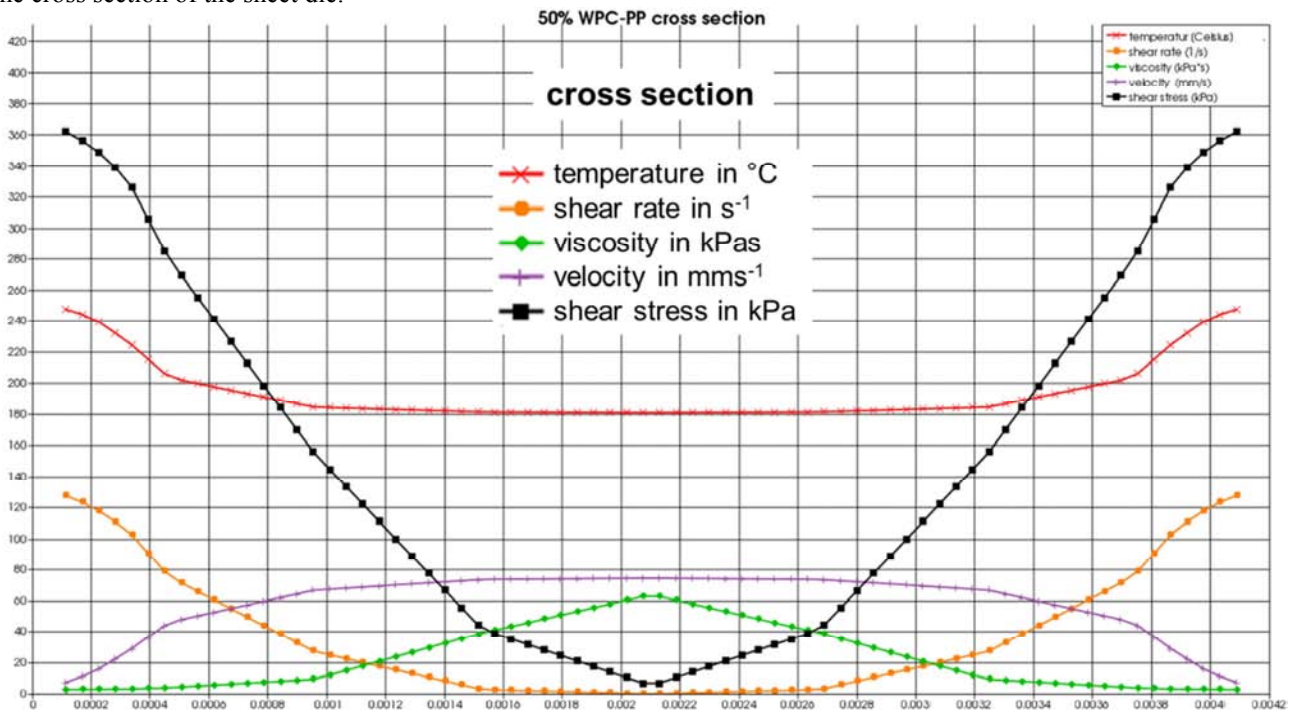


Figure 14. The distribution of the temperature, of the shear rate, of the viscosity, of the velocity and of the shear stress in the cross section of the sheet die for the PP based WPC melt with 50 weight %,  $T = 180^{\circ}\text{C}$ .

One can recognize the high wall shear rates and wall shear stresses which lead to the high temperatures in the wall area of the sheet die.

The velocity distribution at the sheet die exit is shown in figure 15. The deviation of the velocity in the middle of the sheet die is less than 7%.

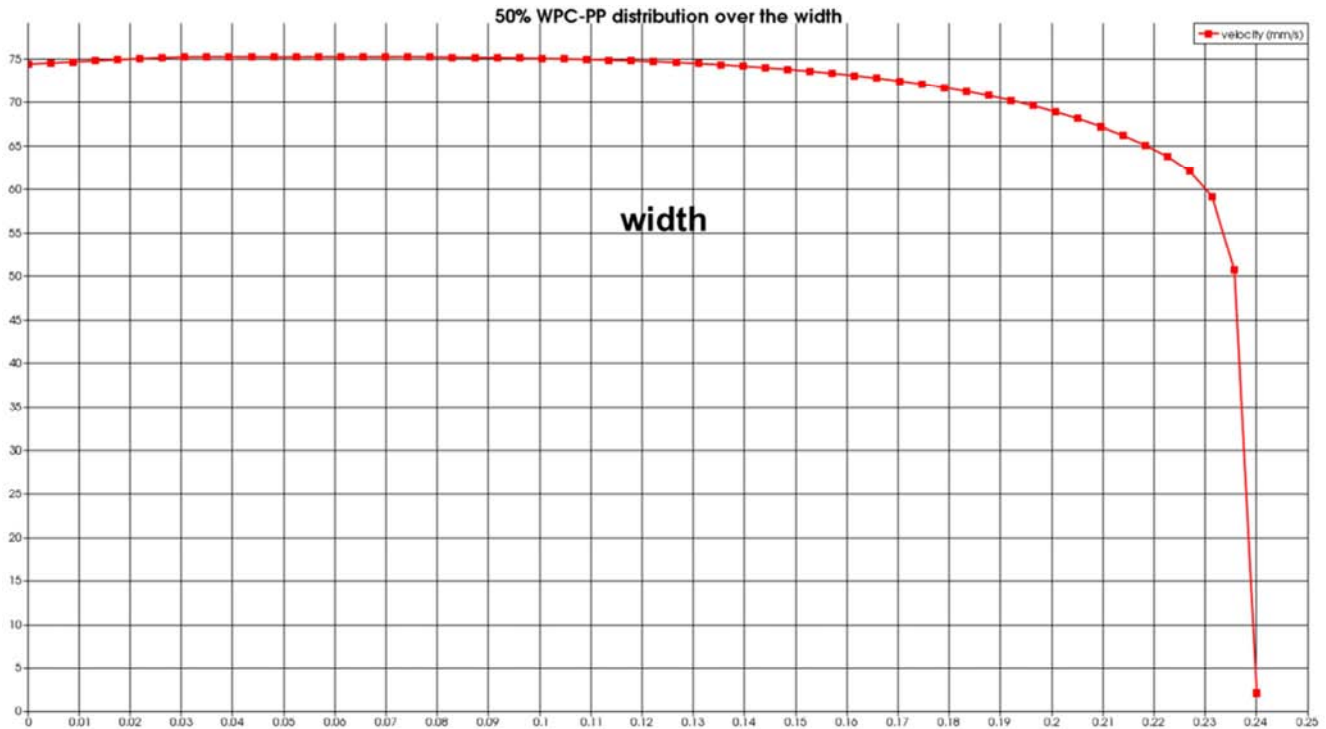


Figure 15. The velocity distribution at the exit of the sheet die across the width for the PP based WPC melt with 50 weight %,  $T = 200^{\circ}\text{C}$ .

Figure 16 shows the average residence time distribution of the PP based WPC melt over the sheet die width. It is widely uniformly distributed and short, so that thermal decomposition is avoided.

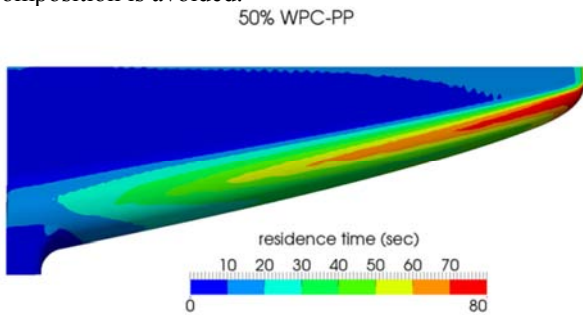


Figure 16. The average residence time distribution in the sheet die for the PP based WPC melt with 50 weight %,  $T = 200^{\circ}\text{C}$ .

## 5. Conclusion

The CARPOW law allows the calculation of the shear flow for melts with an increasing viscosity by decreasing shear rates. The influence of the parameters  $d$ ,  $n$ ,  $a$ ,  $b$  and  $c$  of the CARPOW law on the pressure drop, the shear rate, the shear stress and the velocity distribution is calculated.

The design of the extrusion tools with numerical calculation methods has many advantages. One can see details that are not clear with conventional design methods. In particular, the shear rate at the wall of the flow channel is a sensitive indicator of the quality of the design of the extrusion tool (cleaning flow). Color change, residence time,

temperature increase and pressure drop can be optimized. The design of a flow channel for a wide range of gel contents or filler contents is possible.

## References

- [1] Ostwald, W., Über die Geschwindigkeitsfunktion der Viskosität disperser Systeme, *Kolloid-Z.* 36, (1925), S.99-117.
- [2] Münstedt, H., Viskositätsdaten von Kunststoffen, *Kunststoffe* 68, Nr. 2, (1978), S. 92-98.
- [3] Carreau, P. J., Rheological equations from molecular network theories, Dissertation University of Wisconsin, (1968), DOI: 10.1122/1.549276.
- [4] Fritz, H. G., Geiger, K., Rheologische, thermodynamische und tribologische Grundlagen, Stoffgesetze, Daten für die Auslegung von Extrudern, *Handbuch der Extrudertechnik*, Herausgeber: F. Hensen, W. Knappe und H. Potente, Carl-Hanser-Verlag, München, (1989), S. 14-77.
- [5] Geiger, K., Kühnle, H., Analytische Berechnung einfacher Scherströmungen aufgrund eines Fließansatzes von Carreauschem Typ, *Rheol. Acta*, 23, (1984), S. 355-367.
- [6] N. N., Softwarepaket MATLAB, Mathworks Inc., (2014).
- [7] Rabinowitsch, B., Über die Viskosität und Elastizität von Solen, *Z. Phys. Chem.*, 145, (1929), S. 1-27.
- [8] Anderlik, R., Fritz, H. G., Compounding of Thermoplastic Elastomers using Organosilanes, *Intern. Polymer Processing VII*, 3, 1992, S. 212-217, DOI: 10.3139/217.920212.

- [9] Cox, W. P., Merz, E. H., Correlation of Dynamic and Steady Flow Viscosities, *J. Polym. Sci.*, 28, (1958), S. 619-622, DOI: 10.1002/pol.1958.1202811812.
- [10] Geiger, K., Martin, G. A., Sobotta, A., Relaxationszonen in Werkzeugen, *Kunststoffe*, 6, (2011). S. 44-49.
- [11] Geiger, K., Ein neues heuristisches Fließgesetz, 21. Stuttgarter Kunststoff-Kolloquium, 2009, 3/V4, S. 1-15.
- [12] Perdikoulis, J., Shear Stress vs. Shear Rate as Flow Channel Design Criteria, ANTEC 2017, Anaheim CA, 8.-10. Mai 2017.
- [13] Musialek, M., Beitrag zur Vorhersage des Fließverhaltens hochgefüllter Kunststoffe, Dissertation, Universität Stuttgart, 2016.
- [14] Mazzanti, V., Rheology of Wood Polymer Composites, Dottorato di Ricerca in "Scienze Dell'Ingegneria", Iniversita degli Studi di Ferrara, 2018.
- [15] Laufer, N., Hansmann, H., Koch, M., Rheological Characterisation of the Flow Behaviour of Wood Plastic Composites in Consideration of Different Volume Fraction of Wood, 2nd International Conference on Rheology and Modeling of Materials (IC-RMM2), IOP Conf. Series: Journal of Physics: Conf. Series 790, 2017.
- [16] de Santi, C. R., Hage, E. jr., Vlachopoulos, J., Correa, C. A., Profile Extrusion of WPC's Supported by Rheological and Simulation Data, Anais do 10º Congresso Brasileiro de Polimeros, Foz do Iguacu, 2009.